Dalton Transactions

ROYAL SOCIETY OF CHEMISTRY

PAPER

View Article Online
View Journal | View Issue

Cite this: *Dalton Trans.*, 2025, **54**, 10574

Design of new thorium nuclear clock materials based on polyatomic ions†

Harry W. T. Morgan, *[a,b] Hoang Bao Tran Tan, [c,d] Andrei Derevianko, [c] Ricky Elwell, [e] James E. S. Terhune, [e] Eric R. Hudson [e] and Anastassia N. Alexandrova *[a]

Compounds of polyatomic anions are investigated theoretically as hosts for thorium in nuclear clock devices. The ^{229}Th nucleus has an excited state at 8.355 eV which can be reached using a VUV laser as demonstrated in recent experiments. Incorporating ^{229}Th into a host crystal is an essential step towards developing an ultra-stable nuclear clock. To be a suitable host, a material must have a band gap larger than the nuclear transition frequency. Thus, most research to date has focused on fluorides like $LiSrAlF_6$ and CaF_2, for they feature ionic bonding and large band gaps. Ionicity of chemical bonding can be pushed to its limits by superhalogens – polyatomic anions whose electron affinity can be greater than that of the halogens. An additional concern for fluorides is the presence of ^{19}F nuclear spins in the material that can couple to the spin of the ^{229}Th, detrimental to clock performance. In this work we investigate salts containing superhalogen anions, with the goal of identifying promising new hosts for ^{229}Th clocks. Specifically, we investigate compounds of Ca, Sr, and Ba with three anions – BF_4^-, ClO_4^-, and SO_4^{2-}. By computing the electronic properties of the pure and thorium-doped materials, we predict that $M(BF_4)_2$ have the widest band gaps, making them a promising material class. On the other hand, MSO_4 could produce the most accurate clocks by eliminating inhomogeneous broadening due to nuclear spin interactions. These results may guide experimental searches for new ^{229}Th clock materials and offer new opportunities to study this unique nuclear transition in the solid state.

Received 26th March 2025,
Accepted 16th June 2025

DOI: 10.1039/d5dt00736d

rsc.li/dalton

1 Introduction

Accurate chronometry is essential for fundamental science, precise physical measurements, and communication and navigation technology. Clocks more precise than the current state-of-the-art could even open up the field of relativistic geodesy, using gravitational redshift of the clock frequency to predict earthquakes and volcanic eruptions.[1,2] One such clock could be the thorium nuclear clock. The ^{229}Th isotope has a nuclear excited state at 8.4 eV, similar to the states probed in Mössbauer spectroscopy but at a fraction of the energy, with an extremely long lifetime and narrow transition linewidth.[3] In a solid-state clock, a large number of Th nuclei are interrogated simultaneously, so a given level of accuracy can be attained quickly, allowing rapid measurements. In the parlance of clock technology, solid-state clocks are exceptionally stable. Since the excitation primarily involves the nucleus, it is expected to be less susceptible to environmental perturbations than traditional atomic clocks based on electronic transitions, such as the hyperfine transition in atomic caesium.[4] Furthermore, a solid-state clock could be more practical "in the field" than systems involving atomic vapour or trapped ions. Laser excitation of the ^{229}Th nucleus has recently been demonstrated in thorium-doped single crystals of $LiSrAlF_6$ and CaF_2,[5–7] and in ThF_4 thin films.[8]

One essential requirement for a candidate host material is that it must have a band gap larger than the nuclear excitation energy of 8.4 eV; if it does not then the incident laser radiation will be absorbed by the electrons of the material rather than the ^{229}Th nuclei. Research so far has focused largely on s-block metal fluorides such as MgF_2, CaF_2, $LiCaAlF_6$, and $LiSrAlF_6$,[5,6,9–14] and stoichiometric thorium fluorides.[8,15] Because those metals have low ionization energies and fluo-

[a]*Department of Chemistry and Biochemistry, University of California, Los Angeles, 607 Charles E Young Drive, Los Angeles, California 90095, USA. E-mail: harry.morgan@manchester.ac.uk, ana@chem.ucla.edu*
[b]*Department of Chemistry, University of Manchester, Oxford Road, Manchester M13 9PL, UK*
[c]*Department of Physics, University of Nevada, Reno, Nevada 89557, USA*
[d]*Los Alamos National Laboratory, P.O. Box 1663, Los Alamos, New Mexico 87545, USA*
[e]*Department of Physics and Astronomy, University of California, Los Angeles, California 90095, USA*

†Electronic supplementary information (ESI) available: Details of methods and additional results and figures as described in the text, and DFT-optimized geometries in VASP POSCAR format. See DOI: https://doi.org/10.1039/d5dt00736d

rine has a large electron affinity, fluorides have large band gaps, reflecting the amount of energy required to move an electron from F − to a M^{q+} cation. In searching for 'simple' ionic compounds for clock applications, we are almost completely restricted to fluorides because no other element is electronegative enough to produce such a large band gap.[16]

Chemistry can reveal new directions in the search for clock materials. "Superhalogens" are molecular species with electron affinities greater than halogen atoms, so we expect compounds of their anions with s-block metals to have the required band gaps.[17,18] Commonly encountered superhalogen anions include BF_4^-, PF_6^-, and ClO_4^-, which are often used as non-coordinating anions in solution or in ionic liquids.[19] The large ionization energies stem from delocalization of the negative charge over multiple electronegative atoms, and strong covalent bonding. We anticipate that the large ionization energies of the anion will correspond to large band gaps in corresponding salts.

Here we investigate three groups of compounds by studying the electronic properties of the pure phases and thorium defects: metal sulfates MSO_4, perchlorates $M(ClO_4)_2$, and tetrafluoroborates $M(BF_4)_2$ (M = Ca, Sr, Ba). All three ions have strong covalent bonding and charge delocalization, so we expect them to produce large-gap salts. Strictly, SO_4^{2-} is not a superhalogen because its double negative charge gives it a negative first ionization energy in the gas phase, but in an ionic crystal it is similar to ClO_4^-.[20] Most of the compounds have been synthesized and characterized in anhydrous and hydrated forms.[21–32] We expect the hydrates to have smaller band gaps due to the additional electronic states introduced by water, so we have chosen to focus on the anhydrous materials. For each group we will begin by computing the bulk band gaps to determine whether the host is transparent to photons at the nuclear excitation energy, and then perform thorium doping studies to find the thorium defect electronic properties, specifically 5f orbital energies and markers of Th-anion covalency. We will then determine the viability of polyatomic anions in thorium clocks and identify the best candidates for experimental study.

2 Methods

DFT calculations were performed with VASP,[33] version 6.4.2, using the PAW[34] method with a plane-wave cutoff of 500 eV and a spin-restricted formalism. The PBE[35] functional was used for structural optimizations and defect formation energies, and the modified Becke–Johnson (MBJ)[36,37] and HSE06[38,39] functionals were used for electronic properties. Structural optimizations were performed using Monkhorst–Pack *k*-meshes with point spacings of 0.03 $Å^{-1}$ for bulk materials and 0.04 $Å^{-1}$ for the defect supercells. Structures were visualized using VESTA.[40] MBJ calculations used point spacings of 0.02 $Å^{-1}$ for the bulk materials and 0.025 $Å^{-1}$ for the defect supercells. In our defect models the thorium atom replaces a metal cation and a neighbouring cation vacancy is created to balance the charge. It is also possible that the charge could be compensated by additional anions, but we have not explored that possibility here for consistency between materials and because we cannot identify what those anions might be due to uncertainties in the synthetic methods.

3 Results

3.1 Undoped phases

3.1.1 MSO_4 sulfates. A problem with the fluoride clocks is magnetic dipolar coupling between ^{229}Th and ^{19}F, which causes inhomogeneous broadening of the nuclear transition.[4] The effect is similar to the peak broadening seen in solid-state NMR. The common isotopes of S and O are $I = 0$ nuclei, so the sulfates offer a route to a zero-nuclear-spin clock that may be six orders of magnitude more stable than a fluoride clock.[4,8,41] Thorium sulfate $Th(SO_4)_2$ is also of considerable interest as a clock material, but will not be discussed here because it is stoichiometric and so must be treated with different methods.[41–44] $SrSO_4$ and $BaSO_4$ adopt the same structure (space group *Pnma*), but $CaSO_4$ is slightly different (space group *Amma*) (Fig. 1).[30,32] The band gaps of these sulfates were computed with the MBJ and HSE06 density functionals and are reported in Table 1. Projected density of states (PDOS) plots for the elements show that the band gap in all these materials is a charge transfer from O 2p to M^{2+} d (see ESI†). Which of these datasets is more trustworthy is difficult to say; HSE06 is typically considered the "better" method for most applications but is known to underestimate large band gaps, while MBJ is specialized for band gaps.[15,36,45–47] The chemical properties of sulfates are also favourable in that they are unreactive, non-toxic, and somewhat hygroscopic but easily dried. We believe

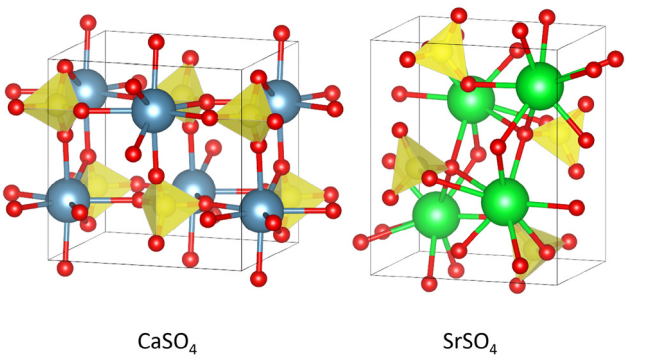

Fig. 1 Unit cells of sulfates $CaSO_4$ and $SrSO_4$.

Table 1 Computed band gaps of bulk sulfates

	MBJ (eV)	HSE06 (eV)
$CaSO_4$	8.53	7.91
$SrSO_4$	8.71	8.07
$BaSO_4$	8.40	8.02

that these results motivate further experimental study of these sulfates, specifically the optical properties of very pure and thorium-doped crystals. Previous studies have found that optical band gaps depend on purity and morphology, so it is plausible that high-purity single crystals could be used as thorium hosts.[48–50]

3.1.2 $M(ClO_4)_2$ perchlorates. The $M(ClO_4)_2$ perchlorates (M = Ca, Sr, Ba) were studied by the same procedure. The structures are shown in (Fig. 2) ($Ca(ClO_4)_2$ and $Sr(ClO_4)_2$ have the same structure).[27,28] The structures are shown in the ESI† and band gaps are given in Table 2. The perchlorates appear to be similar to each other and have slightly smaller band gaps than the sulfates. That is a surprising result because ClO_4^- is a monoanion while SO_4^{2-} is a dianion, so we might expect excitation of an electron from SO_4^{2-} to be easier. PDOS plots for the elements, in the ESI,† show that the band gap in all these materials is a charge transfer from O 2p to M^{2+} d, the same as in the sulfates. Chlorine has two common isotopes, ^{35}Cl and ^{37}Cl, both of which are $I = \frac{3}{2}$ nuclei. A perchlorate-based clock would therefore suffer from nuclear spin broadening, but possibly not as much as a fluoride-based clock because in a perchlorate only one fifth of the anion atoms are spin-active and because the closest nuclei to ^{229}Th are $I = 0$. Furthermore, perchlorates are very hygroscopic, deliquescent,[51] and oxidizing, making them comparatively difficult to handle experimentally. Based on the properties of the bulk materials, the sulfates appear to be better candidates.

3.1.3 $M(BF_4)_2$ tetrafluoroborates. The pure $M(BF_4)_2$ phases do not all have the same crystal structure: $Mg(BF_4)_2$ exists only as a hydrate; $Ca(BF_4)_2$ and $Sr(BF_4)_2$ crystallize in the *Pcba* space group;[22,23] and $Ba(BF_4)_2$ adopts a *C*2/*m* structure.[22] We have optimized all four compounds in the *Pcba* structure for maximal comparability. The results for $Mg(BF_4)_2$ can be found in the ESI† since this phase probably cannot be stabilized. We also optimized $Ba(BF_4)_2$ in the *C*2/*m* and $P2_1/c$ structures, finding *C*2/*m* to be the lowest energy structure, in agreement with experiment, then *Pcba* at +0.041 eV f.u.$^{-1}$, and then $P2_1/c$ at +0.159 eV – we will not consider the $P2_1/c$ structure any further.

Table 2 Computed gaps of bulk perchlorates

	MBJ (eV)	HSE06 (eV)
$Ca(ClO_4)_2$	7.82	7.86
$Sr(ClO_4)_2$	8.39	7.84
$Ba(ClO_4)_2$	7.72	7.63

The *Pcba* structure puts the metal cations into 8-coordinate square antiprismatic geometry and *C*2/*m*-$Ba(BF_4)_2$ features 10-coordinate BaF_{10} pentagonal antiprisms, as shown in Fig. 2.

The computed band gaps are all larger than 10 eV, significantly larger than the band gaps of the fluorides, perchlorates and sulfates, supporting our hypothesis that superhalogen salts are excellent candidates for nuclear clocks. Full results are given in Table 3. PDOS plots in the ESI† show that the band gap in these materials is a charge transfer from F − 2p to M^{2+} d.

3.2 Thorium-doped phases

We modelled thorium-doped phases by replacing an M^{2+} atom by Th^{4+} and removing a second M^{2+} to balance the charge. Note that these charge states are dictated by the typical chemistry of the elements and are not enforced in the calculations. Supercells of the hosts were used to reduce unphysical Th–Th interactions such that all Th–Th distances were 11 Å or more. Optimized structures and pictures of the thorium local coordination environments are in the ESI.† The thorium ions are 8- or 9-coordinate across all host material types, with unsymmetrical coordination geometries due to the electrostatic inter-

Table 3 Band gaps of bulk metal tetrafluoroborates computed with the MBJ and HSE06 functionals

Material	MBJ (eV)	HSE06 (eV)
$Ca(BF_4)_2$	10.59	10.78
$Sr(BF_4)_2$	12.01	10.59
$Ba(BF_4)_2$ *Pcba*	11.05.	10.45
$Ba(BF_4)_2$ *C*2/*m*	10.45	10.53

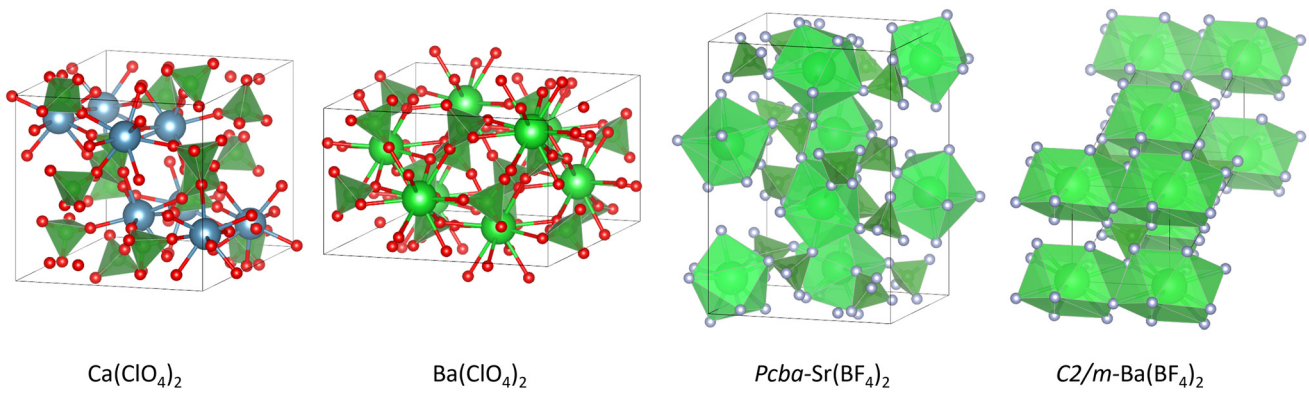

Fig. 2 Optimized unit cells of $Ca(ClO_4)_2$, $Ba(ClO_4)_2$, *Pcba*-$Sr(BF_4)_2$ (high square antiprismatic SrF_8), and *C*2/*m*-$Ba(BF_4)$ (showing pentagonal antiprismatic BaF_{10}).

action between Th^{4+} and the anions. Most anions coordinate in a monodentate mode, though bidentate coordination can be found for all anions and is most common in the sulfates.

For the tetrafluoroborates we computed defect formation energies by balancing the thorium doping reaction with binary metal fluorides, and for sulfates we computed defect formation energies by a reaction between metal sulfates. The results, in Tables S1 and S2,† show that the lowest defect formation energies in tetrafluoroborates are found in $Sr(BF_4)_2$ and $Ba(BF_4)_2$, and the lowest in sulfates is found in $SrSO_4$. Strontium hosts therefore appear particularly good for thorium doping. f-element doping of sulfates is well-established because similar systems (*e.g.* $Dy:CaSO_4$) are used for radiation dosimetry.[52]

The thorium PDOS plots for $Th:SrSO_4$, $Th:Sr(ClO_4)_2$, and $Th:Sr(BF_4)_2$ are shown in Fig. 3. The electronic character of thorium is similar in all three materials. The 5f orbitals form narrow peaks around 5 eV and the 6d orbitals appear as sharp peaks at higher energies. The energies of the 5f peak are highest in $Sr(BF_4)_2$ and lowest in $Sr(ClO_4)_2$, weakly matching the trend in the band gaps of the host crystals. The 6d orbitals form a set of sharp peaks at higher energies, mixing into the conduction band in $SrSO_4$ and $Sr(ClO_4)_2$. Thorium makes no contribution to the upper part of the valence band, appearing only in states below 1 eV, so the lowest thorium-centered electronic transitions are actually higher than the 5f energy relative to E_F. This is a characteristic feature of cells containing cation vacancies because undercoordinated anions form the top of the valence band.

3.2.1 Internal conversion. For the clock to work, the ^{229}Th nuclei must decay radiatively rather than decaying by internal conversion (IC), where energy is transferred to the electrons.[12,53] For IC to be energetically possible, there must be electronic excited states below 8.4 eV. For it to be fast, relative to radiative decay, the electronic states have to overlap with the nuclear wavefunction. A sophisticated theoretical treatment of the IC rate based on Fermi's golden rule has been developed.[53]

The electronic part of IC is transfer of an electron from the anions to the vacant Th^{4+} 5f orbitals, so IC will be fast if there is strong orbital hybridization between Th 5f and the anions, and slow if there is weak hybridization. The thorium 5f PDOS in the valence band shows the extent of hybridization. For a quantitative comparison between compounds we integrate this PDOS over the valence band to give the "IPDOS" (integrated projected density of states), which is equivalent to the population of the Th 5f shell. Another benefit of the IPDOS is that it is not sensitive to the energies of the unoccupied 5f orbitals, which are subject to well-known DFT errors.

Th 5f IPDOSs for all compounds in this study can be found in Table S2.† The values are smallest for the sulfates and highest for the tetrafluoroborates. The IPDOS for $Th:LiSrAlF_6$, for which radiative decay of the nuclear excited state has been observed, is in the same range as the polyatomic anion materials. A second descriptor of hybridization, the width of the 5f peak, is also discussed in the ESI.† The conclusion here is that the orbital hybridization calculations suggest slow IC in thorium-doped sulfates, supporting our conclusion that they are excellent candidates for experimental study.

3.2.2 Cation-disordered phases. So far we have considered materials with a single cation, which we can expect to have minimal crystallographic disorder. We could also consider a solid solution like $Sr_xBa_{1-x}(BF_4)_2$, since mixed metal materials and "high entropy alloys" offer advantages in many technologies.[54–56] In that case the cations (Sr and Ba in $Sr_xBa_{1-x}(BF_4)_2$) may be distributed randomly over the cation sites. Unfortunately, such disorder will severely reduce clock accuracy. The ^{229}Th nuclear transition frequency is influenced by coupling of the nuclear quadrupole moment to the electric field gradient (EFG) at the nucleus. In disordered $Sr_xBa_{1-x}(BF_4)_2$, for example, there will be many different thorium environments, each defined by the arrangement of the nearby Sr^{2+} and Ba^{2+} cations. The resulting variation in transition frequencies can be related to the accuracy of the

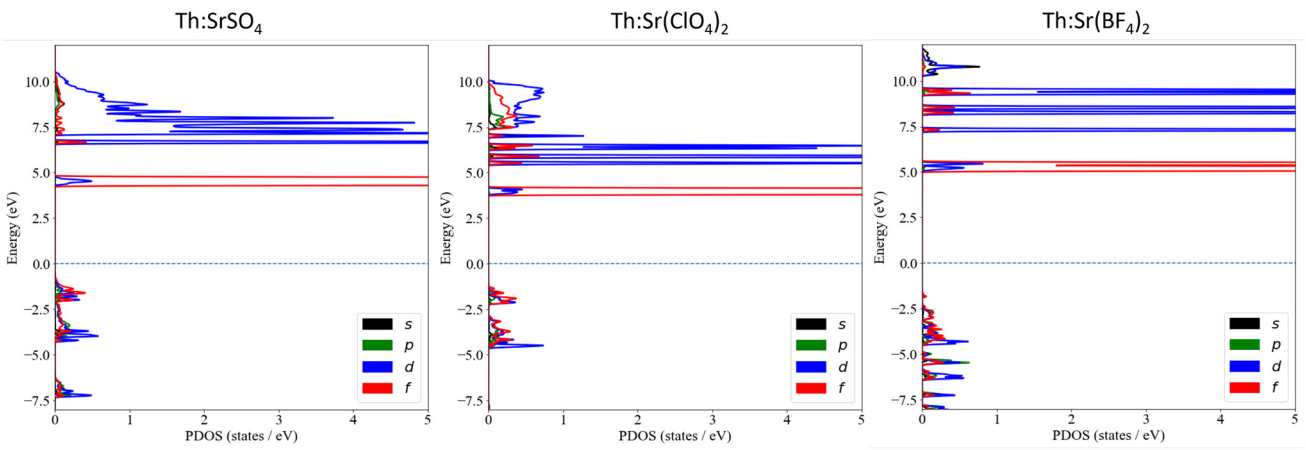

Fig. 3 Thorium projected density of states plots for $Th:SrSO_4$, $Th:Sr(ClO_4)_2$, and $Th:Sr(BF_4)_2$.

clock through the quality factor $Q = \frac{\nu_0}{\Delta\nu}$ where ν_0 is the transition frequency and $\Delta\nu$ is the linewidth. We have estimated $Q = 5 \times 10^7$ for disordered $Sr_xBa_{1-x}(BF_4)_2$, which is comparable to the accuracy of quartz oscillators. The details of our estimation can be found in the ESI.† This result suggests that ordered crystalline materials will be required for accurate crystal clocks.

4 Conclusions

In conclusion, we predict alkaline earth tetrafluoroborates $M(BF_4)_2$ and sulfates MSO_4 (M = Ca, Sr, Ba) to be excellent candidate materials for solid-state ^{229}Th nuclear clocks. Inspired by non-coordinating anions in solution-phase chemistry and the concept of superhalogens, we identified the BF_4^-, ClO_4^-, and SO_4^{2-} ions as having the right electronic properties for crystal clocks: they have large ionization potentials, giving a large band gaps in salts, and strong internal covalent bonds, minimizing Th–X covalency in crystals. Both of these effects combine to give a good opportunity for observing radiative decay of the isomeric state of ^{229}Th after laser excitation.

The largest host band gaps are possessed by $M(BF_4)_2$, so they should all be transparent to the VUV laser. All have similar Th 5f energies, but $Ba(BF_4)_2$ has the lowest markers of Th–F covalency, implying a desirably low IC rate. $Sr(BF_4)_2$ and $Ba(BF_4)_2$ have the lowest defect formation energies so we might expect a higher concentration of thorium than in $Ca(BF_4)_2$. Overall, $Ba(BF_4)_2$ is therefore the best candidate for laser excitation and radiative decay of the nucleus. The tetrafluoroborate series may offer exploration of the effects of small electronic changes on nuclear decay processes.

The sulfates have a major advantage for clock accuracy in being nuclear-spin-free. The absence of nuclear spins could make a sulfate clock more accurate than a fluoride clock by six orders of magnitude. We cannot be certain of which sulfates are transparent to the exciting radiation, based on computations of the band gaps, so experimental measurements of the optical band gaps of high-purity single crystals are needed. The perchlorates are inferior to the sulfates in several ways: they contain nuclear spins on chlorine; they have smaller band gaps and lower Th 5f energies; and they have undesirable chemical properties.

We have also found that ordered materials are likely to be a necessity for any of the cutting-edge applications proposed for nuclear clocks because the variation in electric field gradients created by cation disorder reduces the accuracy of the clock by many orders of magnitude. These results point to a broad class of materials, featuring polyatomic anions, that can provide us with new opportunities to study ^{229}Th photophysics and that may outperform metal fluorides in crystal clocks.

Author contributions

H. W. T. Morgan: conceptualization; data curation; formal analysis; investigation; methodology; project administration; resources; visualization; writing – original draft; writing – review & editing. H. B. Tran Tan: formal analysis; investigation; methodology; writing – review & editing. A. Derevianko: data curation; formal analysis; funding acquisition; investigation; methodology; project administration; resources; supervision; writing – review & editing. R. Elwell: formal analysis; investigation; methodology; writing – review & editing. J. E. S. Terhune: formal analysis; investigation; methodology; writing – review & editing. E. R. Hudson: data curation; formal analysis; funding acquisition; investigation; methodology; project administration; resources; supervision; writing – review & editing. A. N. Alexandrova: conceptualization; data curation; formal analysis; funding acquisition; investigation; methodology; project administration; supervision; resources; writing – review & editing.

Conflicts of interest

E.R.H. has US Patent No. 63/757422 pending.

Data availability

The data supporting this article have been included as part of the ESI.†

Acknowledgements

This work was supported by NSF awards PHYS-2013011, PHY-2207546, and PHYS-2412982, and ARO award W911NF-11-1-0369. ERH acknowledges institutional support by the NSF QLCI Award OMA-2016245. This work used Bridges-2 at Pittsburgh Supercomputing Center through allocation PHY230110 from the ACCESS program, which is supported by NSF grants #2138259, #2138286, #2138307, #2137603, and #2138296.

References

1 J. Müller, D. Dirkx, S. Kopeikin, G. Lion, I. Panet, G. Petit and P. Visser, *Space Sci. Rev.*, 2018, **214**, 5.
2 T. Mehlstäubler, G. Grosche, C. Lisdat, P. Schmidt and H. Denker, *Rep. Prog. Phys.*, 2018, **81**, 064401.
3 C. Campbell, A. Radnaev, A. Kuzmich, V. Dzuba, V. Flambaum and A. Derevianko, *Phys. Rev. Lett.*, 2012, **108**, 120802.
4 W. Rellergert, D. DeMille, R. Greco, M. Hehlen, J. Torgerson and E. Hudson, *Phys. Rev. Lett.*, 2010, **104**, 200802.
5 R. Elwell, C. Schneider, J. Jeet, J. Terhune, H. Morgan, A. Alexandrova, H. Tan, A. Derevianko and E. Hudson, *Phys. Rev. Lett.*, 2024, **133**, 013201.
6 J. Tiedau, M. Okhapkin, K. Zhang, J. Thielking, G. Zitzer, E. Peik, F. Schaden, T. Pronebner, I. Morawetz, L. De Col,

F. Schneider, A. Leitner, M. Pressler, G. Kazakov, K. Beeks, T. Sikorsky and T. Schumm, *Phys. Rev. Lett.*, 2024, **132**, 182501.
7 C. Zhang, T. Ooi, J. S. Higgins, J. F. Doyle, L. von der Wense, K. Beeks, A. Leitner, G. A. Kazakov, P. Li, P. G. Thirolf, T. Schumm and J. Ye, *Nature*, 2024, **633**, 63–70.
8 C. K. Zhang, L. von der Wense, J. F. Doyle, J. S. Higgins, T. Ooi, H. U. Friebel, J. Ye, R. Elwell, J. E. S. Terhune, H. W. T. Morgan, A. N. Alexandrova, H. B. T. Tan, A. Derevianko and E. R. Hudson, *Nature*, 2024, **636**, 603–608.
9 M. Pimon, J. Gugler, P. Mohn, G. A. Kazakov, N. Mauser and T. Schumm, *J. Phys.:Condens. Matter*, 2020, **32**, 255503.
10 M. Pimon, P. Mohn and T. Schumm, *Adv. Theory Simul.*, 2022, **5**, 2200185.
11 B. S. Nickerson, M. Pimon, P. V. Bilous, J. Gugler, K. Beeks, T. Sikorsky, P. Mohn, T. Schumm and A. Pálffy, *Phys. Rev. Lett.*, 2020, **125**, 032501.
12 B. S. Nickerson, M. Pimon, P. V. Bilous, J. Gugler, G. A. Kazakov, T. Sikorsky, K. Beeks, A. Grüneis, T. Schumm and A. Pálffy, *Phys. Rev. A*, 2021, **103**, 053120.
13 Q. Gong, S. Tao, S. Li, G. Deng, C. Zhao and Y. Hang, *Phys. Rev. A*, 2024, **109**, 033109.
14 S. V. Pineda, P. Chhetri, S. Bara, Y. Elskens, S. Casci, A. N. Alexandrova, M. Au, M. Athanasakis-Kaklamanakis, M. Bartokos, K. Beeks, C. Bernerd, A. Claessens, K. Chrysalidis, T. E. Cocolios, J. G. Correia, H. De Witte, R. Elwell, R. Ferrer, R. Heinke, E. R. Hudson, F. Ivandikov, Y. Kudryavtsev, U. Köster, S. Kraemer, M. Laatiaoui, R. Lica, C. Merckling, I. Morawetz, H. W. T. Morgan, D. Moritz, L. M. C. Pereira, S. Raeder, S. Rothe, F. Schaden, K. Scharl, T. Schumm, S. Stegemann, J. Terhune, P. G. Thirolf, S. M. Tunhuma, P. Van Den Bergh, P. Van Duppen, A. Vantomme, U. Wahl and Z. Yue, *Phys. Rev. Res.*, 2025, **7**, 013052.
15 J. Ellis, X. Wen and R. Martin, *Inorg. Chem.*, 2014, **53**, 6769–6774.
16 A. L. Allred, *J. Inorg. Nucl. Chem.*, 1961, **17**, 215–221.
17 A. Srivastava, *Chem. Commun.*, 2023, **59**, 5943–5960.
18 G. Gutsev and A. Boldyrev, *Chem. Phys.*, 1981, **56**, 277–283.
19 A. Srivastava, A. Kumar and N. Misra, *J. Phys. Chem. A*, 2021, **125**, 2146–2153.
20 S. Nielsen and A. Ejsing, *Chem. Phys. Lett.*, 2007, **441**, 213–215.
21 J. Forero-Saboya, M. Lozinsek and A. Ponrouch, *J. Power Sources Adv.*, 2020, **6**, 100032.
22 T. Bunic, G. Tavcar, E. Goreshnik and B. Zemva, *Acta Crystallogr., Sect. C:Cryst. Struct. Commun.*, 2007, **63**, I75–I76.
23 T. Jordan, B. Dickens, L. Schroeder and W. Brown, *Acta Crystallogr., Sect. B*, 1975, **31**, 669–672.
24 E. Mikuli, E. Szostak and B. Grad, *Phase Transitions*, 2007, **80**, 539–546.
25 E. Goreshnik, A. Vakulka and G. Tavcar, *IUCrData*, 2023, **8**, x230488.
26 D. O. Charkin, S. N. Volkov, L. S. Manelis, A. N. Gosteva, S. M. Aksenov and V. A. Dolgikh, *J. Struct. Chem.*, 2023, **64**, 253–261.
27 J. Hyoung, H. Lee, S. Kim, H. Shin and S. Hong, *Acta Crystallogr., Sect. E:Crystallogr. Commun.*, 2019, **75**, 447–450.
28 J. Lee, J. Kang, S. Lim and S. Hong, *Acta Crystallogr., Sect. E:Crystallogr. Commun.*, 2015, **71**, 588–591.
29 P. Murthy and C. Patel, *J. Inorg. Nucl. Chem.*, 1963, **25**, 310–312.
30 A. Christensen, M. Olesen, Y. Cerenius and T. Jensen, *Chem. Mater.*, 2008, **20**, 2124–2132.
31 A. Lauer, R. Hellmann, G. Montes-Hernandez, N. Findling, W. Ling, T. Epicier, A. Fernandez-Martinez and A. Van Driessche, *J. Chem. Phys.*, 2023, **158**, 054501.
32 M. Krystek, *Phys. Status Solidi A*, 1979, **54**, K133–K135.
33 G. Kresse and J. Furthmuller, *Phys. Rev. B*, 1996, **54**, 11169–11186.
34 P. E. Blochl, *Phys. Rev. B*, 1994, **50**, 17953–17979.
35 J. P. Perdew, K. Burke and M. Ernzerhof, *Phys. Rev. Lett.*, 1996, **77**, 3865–3868.
36 F. Tran and P. Blaha, *Phys. Rev. Lett.*, 2009, **102**, 226401.
37 A. D. Becke and E. R. Johnson, *J. Chem. Phys.*, 2006, **124**, 221101.
38 J. Heyd, G. E. Scuseria and M. Ernzerhof, *J. Chem. Phys.*, 2003, **118**, 8207–8215.
39 A. Krukau, O. Vydrov, A. Izmaylov and G. Scuseria, *J. Chem. Phys.*, 2006, **125**, 224106.
40 K. Momma and F. Izumi, *J. Appl. Crystallogr.*, 2008, **41**, 653–658.
41 H. W. T. Morgan, J. E. S. Terhune, R. Elwell, H. B. T. Tan, U. C. Perera, A. Derevianko, E. R. Hudson and A. N. Alexandrova, A spinless crystal for a high-performance solid-state 229Th nuclear clock, *arXiv*, 2025, 2503.11374, DOI: **10.48550/arXiv.2503.11374**.
42 U. Betke and M. S. Wickleder, *Eur. J. Inorg. Chem.*, 2011, **2012**, 306–317.
43 A. Abrao, A. de Freitas and F. de Carvalho, *J. Alloys Compd.*, 2001, **323**, 53–56.
44 A. Albrecht, G. Sigmon, L. Moore-Shay, R. Wei, C. Dawes, J. Szymanowski and P. Burns, *J. Solid State Chem.*, 2011, **184**, 1591–1597.
45 V. Wang, N. Xu, J. Liu, G. Tang and W. Geng, *Comput. Phys. Commun.*, 2021, **267**, 108033.
46 D. J. Singh, *Phys. Rev. B*, 2010, **82**, 205102.
47 W. Chen and A. Pasquarello, *Phys. Rev. B*, 2012, **86**, 035134.
48 S. H. Jagdale and S. H. Pawar, *Bull. Mater. Sci.*, 1983, **5**, 389–397.
49 A. Kadari, K. Mahi, R. Mostefa, M. Badaoui, A. Mameche and D. Kadri, *J. Alloys Compd.*, 2016, **688**, 32–36.
50 H. Nagabhushana, G. Nagaraju, B. Nagabhushana, C. Shivakumara and R. Chakradhar, *Philos. Mag. Lett.*, 2010, **90**, 289–298.
51 D. Nuding, E. Rivera-Valentin, R. Davis, R. Gough, V. Chevrier and M. Tolbert, *Icarus*, 2014, **243**, 420–428.
52 N. Ingle, S. Omanwar, P. Muthal, S. Dhopte, V. Kondawar, T. Gundurao and S. Moharil, *Radiat. Meas.*, 2008, **43**, 1191–1197.

53 H. W. T. Morgan, H. B. T. Tan, R. Elwell, A. N. Alexandrova, E. R. Hudson and A. Derevianko, Theory of internal conversion of the thorium-229 nuclear isomer in solid-state hosts, *arXiv*, 2024, 2411.15641, DOI: **10.48550/arXiv.2411.15641**.
54 X. Gui, B. Lv and W. Xie, *Chem. Rev.*, 2021, **121**, 2966–2991.
55 E. George, D. Raabe and R. Ritchie, *Nat. Rev. Mater.*, 2019, **4**, 515–534.
56 M. Gawande, R. Pandey and R. Jayaram, *Catal.:Sci. Technol.*, 2012, **2**, 1113–1125.